Supplementary Information (SI) for Materials Chemistry Frontiers.

Supporting Information for

Unveiling Thermal Treatment Effects on Thermomechanical and IR Optical Properties of Chalcogenide Hybrid Inorganic/Organic Polymers

Wonmoo Byun,‡[ab] Jae Hyuk Hwang,‡[a] Jiseok Han,[ac] Juntae Joo,[ac] Sangmin Park,[ad] Woohwa Lee,[a] Hyun Kim,[ad] Chang-Geun Chae,[ad] Sungmin Park,[ad] and Dong-Gyun Kim*[ad]*

[a] Advanced Materials Division, Korea Research Institute of Chemical Technology, 141 Gajeong-ro, Yuseong-gu, Daejeon 34114, Republic of Korea.

[b] Department of Chemical and Biological Engineering, Korea University, 145 Anam-ro, Seongbuk-gu, Seoul 02841, Republic of Korea.

[c] Department of Materials Science and Engineering, Korea University, 145 Anam-ro, Seongbuk-gu, Seoul, 02841, Republic of Korea.

[d] Advanced Materials and Chemical Engineering, KRICT School, University of Science and Technology, 217 Gajeong-ro, Yuseong-gu, Daejeon 34114, Republic of Korea.

*Correspondence to parks@krict.re.kr (Dr. Sungmin Park), and dgkim@krict.re.kr (Dr. Dong-Gyun Kim).

‡These authors contributed equally to this work.

Table of Contents

1. Experimental Section S2
2. Synthesis and Structural Characterization of S80T20 ....S7
3. Thermomechanical Characterization of thermally treated S80T20 ....S8
4. IR Optical Characterization of thermally treated S80T20 ....S17
5. Synthesis and Structural Characterization of S*x*Se*y*T20s S23
6. Thermomechanical and IR Optical Characterization of thermally treated S*x*Se*y*T20s S25
7. References S33

Experimental Section

Materials

Elemental sulfur (ES, ≥99.5%), selenium (Se, powder, 100 mesh, 99.99%), from Sigma-Aldrich, were used as received. Tricyclopentadiene (TCPD, 95%) from ENEOS Corporation, was used as received. All other solvents and reagents were used as received from standard vendors.

Synthesis of poly(S_{80}-*r*-$TCPD_{20}$) (S80T20):

A 50 ml vial equipped with a magnetic stirring bar was filled with elemental sulfur (ES, S_8, 8.0 g, 249.5 mmol) and heated in a thermostated oil bath at 160 °C. After the sulfur was molten and turned into a yellowish liquid, tricyclopentadiene (TCPD, 2.0 g, 10.1 mmol) was then directly added to the molten sulfur medium. The mixture was stirred at 160 °C for 20 min until it became vitrificated. The vial containing the resulting polymer was taken out of the oil bath and naturally cooled down to room temperature. The vial was then quenched by placing it in liquid nitrogen, and then the product was obtained by breaking the vial to yield a yellow solid (91.3 %). CHNS Elemental Analysis of As-synthesized sample*;* C: 14.36 %, H: 1.30 %, S: 84.34 %.

General procedure for the preparation of poly(S_x-*r*-Se_y-*r*-$TCPD_{20}$) (S*x*Se*y*T20):

A 50 ml vial equipped with a magnetic stirring bar was filled with ES (S_8, detailed masses are specified below) and heated in a thermostated oil bath at 160 °C, until it turned into a yellowish liquid molten sulfur. The vial was then transferred to an adjacent thermostatted oil bath (T = 150 °C) in a thermostated oil bath where selenium (Se, detailed masses are specified below) was then directly added to the molten sulfur medium.[S1] When the mixed chalcogens change from opaque black to transparent red (detailed time is specified below), tricyclopentadiene (TCPD, 2.0 g, 10.1 mmol) was then directly added to the mixed chalcogen medium. The mixture was stirred at 150 ℃ for 1 h until it became vitrificated. The vial containing the resulting polymer was taken out of the oil bath and naturally cooled down to room temperature. The vial was then quenched by placing it in liquid nitrogen, and then the product was obtained by breaking the vial.

Synthesis of poly(S_{72}-*r*-Se_{8}-*r*-$TCPD_{20}$) (S72Se8T20):

The inverse vulcanization was carried out following the general procedure shown with ES (7.2 g, 224.5 mmol) and Se (0.8 g, 10.1 mmol) for 30 min to mix the chalcogens, followed by the addition of TCPD (2.0 g, 10.1 mmol) to yield orange solid (90.7 %). CHNS Elemental Analysis of As-synthesized sample*;* C: 16.26 %, H: 1.71 %, S: 74.03 %.

Synthesis of poly(S_{64}-*r*-Se_{16}-*r*-$TCPD_{20}$) (S64Se16T20):

The inverse vulcanization was carried out following the general procedure shown with ES (6.4 g, 199.6 mmol) and Se (1.6 g, 20.3 mmol) for 15 min to mix the chalcogens, followed by the addition of TCPD (2.0 g, 10.1 mmol) to yield red solid (90.8 %). CHNS Elemental Analysis of As-synthesized sample*;* C: 16.25 %, H: 1.62 %, S: 66.13 %.

Synthesis of poly(S_{56}-*r*-Se_{24}-*r*-$TCPD_{20}$) (S56Se24T20):

The inverse vulcanization was carried out following the general procedure shown with ES (5.6

g, 174.6 mmol) and Se (2.4 g, 30.4 mmol) for 5 min to mix the chalcogens, followed by the addition of TCPD (2.0 g, 10.1 mmol) to yield dark red solid (91.4 %). CHNS Elemental Analysis of As-synthesized sample*;* C: 16.39 %, H: 1.57 %, S: 58.04 %.

General procedure of thermal treatment

The S80T20 and S*x*Se*y*T20 samples were thermally treated in an oven under air conditions. All thermal treatments were conducted after the set temperature was reached. After the thermal treatment, samples (or windows) were gradually cooled to room temperature. The thermal treatment time was calculated to include the time during which the windows and films were hot-pressed.

Preparation of free-standing S80T20 film (window)

S80T20 films were prepared by placing the bulk S80T20 into a circular-shaped mold (60 mm (D) × 1 mm (T)), made of Kapton® polyimide films and stainless-steel spacer, and pressing (10 MPa) for 20 min (Figure S13). The samples were subjected to hot-pressing at temperatures of 140°C and 170 °C corresponding to respective post-curing temperatures. The thickness of the film was controlled using the stainless-steel spacer inserted between two polyimide films. After the pressure was removed, the sample was allowed to cool to room temperature before the polyimide film was removed. All films were thermally treated in oven with air condition.

Preparation of free-standing SxSeyT20 film (window)

S*x*Se*y*T20 films were prepared by placing the bulk S*x*Se*y*T20 into a circular-shaped mold (60 mm (D) × 1 mm (T)), made of Kapton® polyimide films and stainless-steel spacer, and pressing (10 MPa) for 20 min. Different processing temperatures were applied for the S*x*Se*y*T20s. 140

and 170 °C were applied for the hot pressing of S*x*Se*y*T20s. The thickness of the film was controlled using the stainless-steel spacer inserted between two polyimide films. After the pressure was removed, the sample was allowed to cool to room temperature before the polyimide film was removed. All films were thermally treated in oven with air condition.

Instrumental and characterization techniques

The elemental content of S80T20, S72Se8T20, S64Se16T20, and S56Se24T20 were analyzed using an elemental analyzer (EA, Flash 2000, Thermo Scientific). Fourier transform infrared (FT-IR) spectra were recorded on a Bruker Alpha II FTIR spectrometer using attenuated total reflectance (ATR) and transmission modes. Gel fraction experiment was performed by placing a small piece (ca. 30 mg) of S80T20, S72Se8T20, S64Se16T20, and S56Se24T20 into a 20 ml vial filled with toluene. After being stored in an oven at room temperature for 24 h, the film was recovered and dried at 60 °C under vacuum for 18 h. Gel fraction (f_g) was calculated using the equation,

$$f_g = W_a / W_d \tag{1}$$

where W_d and W_a are the weights of the dried film before and after the toluene solvent extraction, respectively. The thermal stability of S80T20, S72Se8T20, S64Se16T20, and S56Se24T20 were investigated by thermal gravimetric analysis (TGA) using a TA Instruments TGA Q5000 under a nitrogen atmosphere. The samples were heated from 25 °C to 800 °C at a heating rate of 10 °C min^{-1}. Differential scanning calorimetry (DSC) was run using a TA Instruments DSC Q2000 under a nitrogen atmosphere. Samples with a typical mass of 5–10 mg were encapsulated in sealed aluminum pans. All samples were first heated from –25 °C to 160 °C and then cooled down to –25 °C, which was followed by second heating at a constant rate of 10 °C min^{-1}. Dynamic mechanical analysis (DMA) was performed on a TA Instruments

DMA Q800 with an attached cryo accessory using rectangular-shaped S80T20 and S*x*Se*y*T20 films (ca. 50 mm (L) × 5 mm (W) × 0.5 mm (T)). DMA was conducted in the film tension mode with a 1-Hz frequency, 0.01 % strain, and 0.001-N axial force. The specimens were first cooled from 30 °C to –50 °C and then heated to 130 °C at a constant rate of 5 °C min^{-1} in a nitrogen atmosphere. The crosslinking density (v_e) of the S80T20 and S*x*Se*y*T20s was calculated as

$$v_{\mathrm{e}} = E' / 3RT \tag{2}$$

where E', R, and T denote the storage modulus, universal gas constant, and absolute temperature in the rubbery region (ca. 356.15 K), respectively. Refractive index measurements of S80T20, S72Se8T20, S64Se16T20, and S56Se24T20 films were conducted on a Metricon 2010/M prism coupler at 532 nm, 632.8 nm, and 829 nm. Mid-wave infrared (MWIR) camera (COX640AV, resolution of 640 × 480, 15 μm of pixel pitch, COX) was utilized to capture ambient temperature MWIR (3–5 μm) thermograms. Raman spectra analyses were conducted using the instrument of Bruker FRA 106/S.

Synthesis and Structural Characterization of S80T20

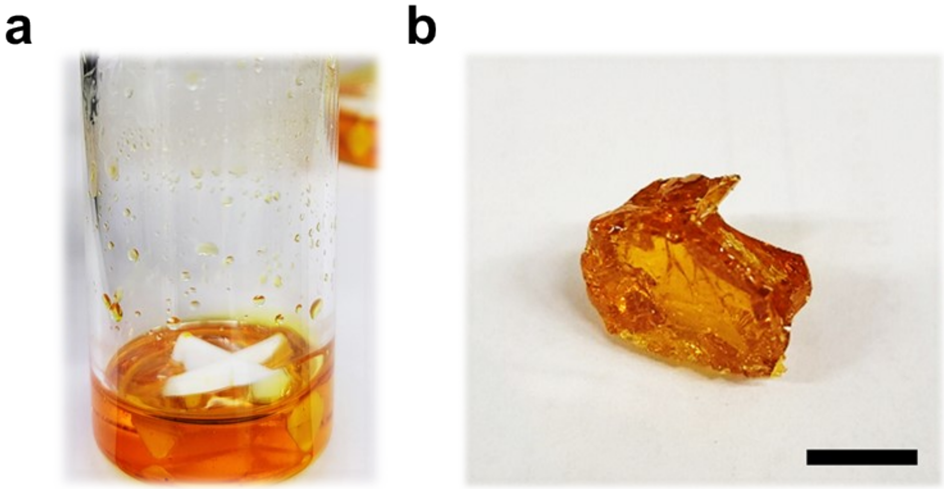

Fig. S1. Digital images of (a) vitrified S80T20 immediately after inverse vulcanization and (b) obtained S80T20 chunk after quenching in liquid nitrogen. Scale bar for the image is 1 cm.

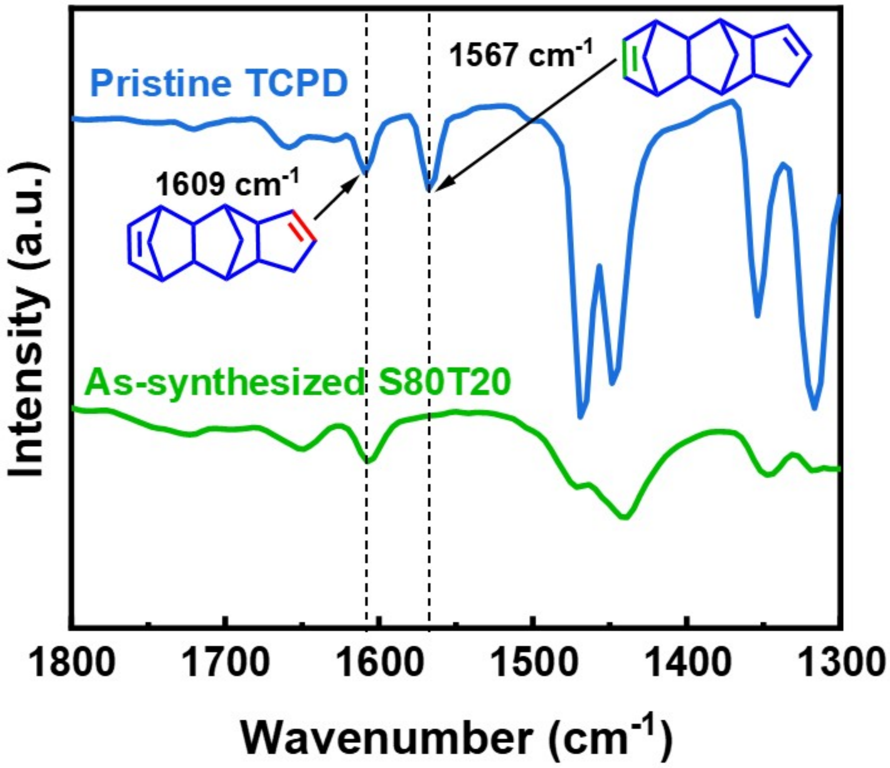

Fig. S2. FT-IR (ATR mode) spectra of TCPD and as-synthesized S80T20.

Thermomechanical Characterization of thermally treated S80T20

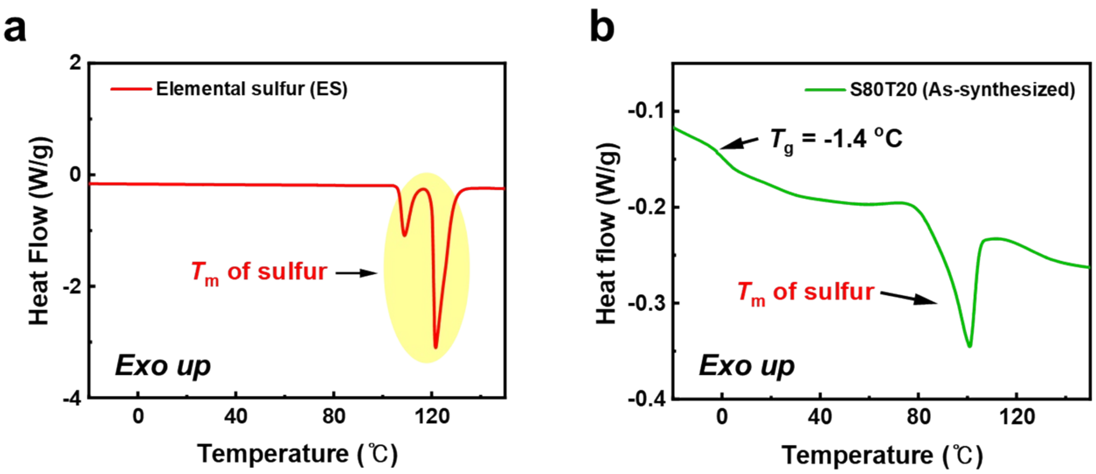

Fig. S3. DSC thermograms of (a) ES and TCPD and (b) as-synthesized S80T20.

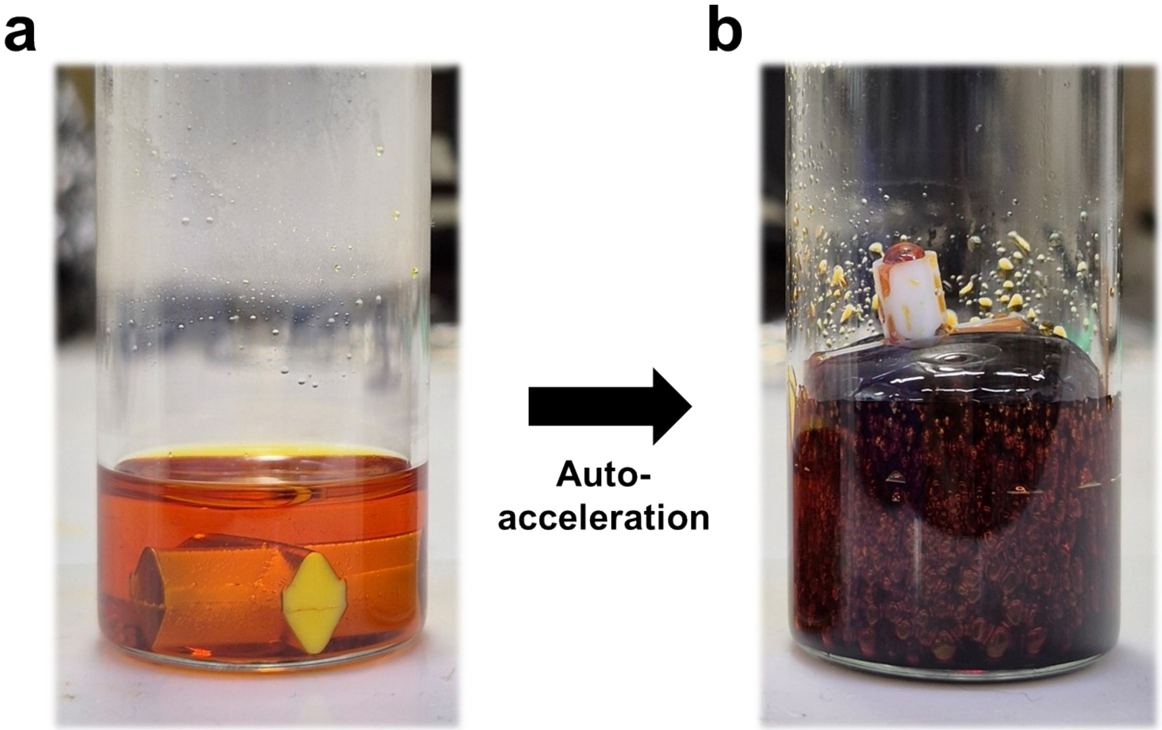

Fig. S4. S80T20 samples of (a) immediately vitrified and (b) auto-accelerated within the vial.

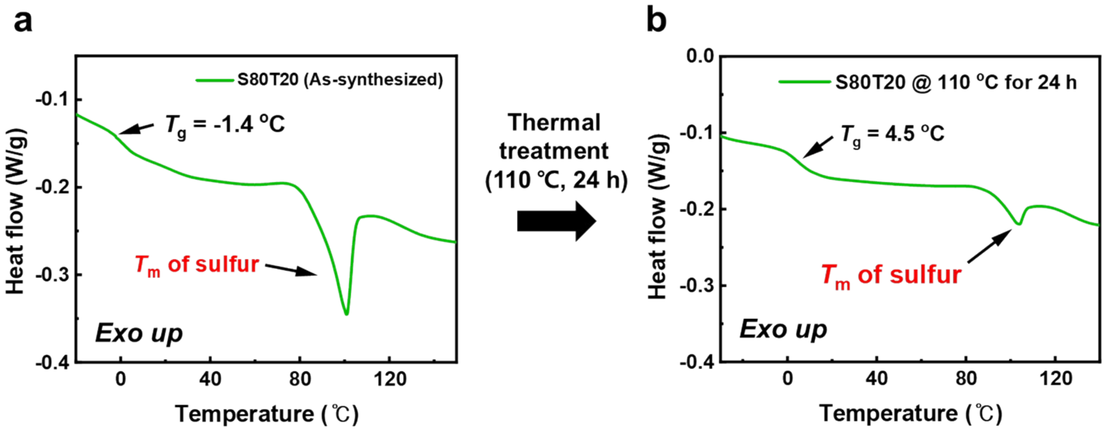

Fig. S5. DSC thermograms of (a) as-synthesized S80T20 and (b) thermally treated S80T20 at 110 °C for 24 h.

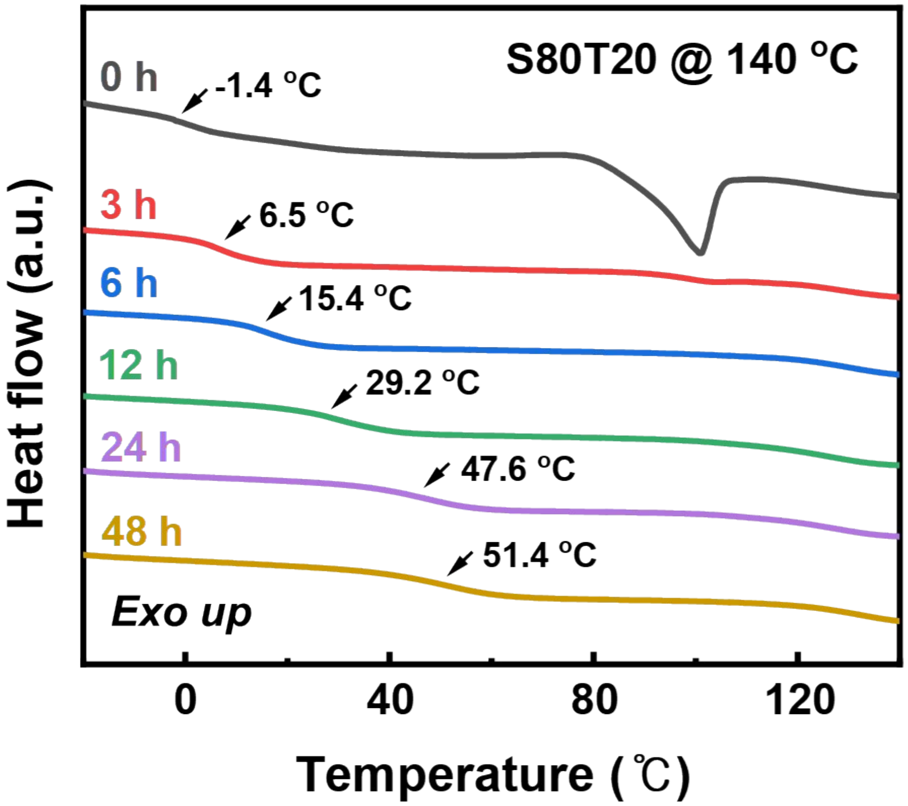

Fig. S6. DSC thermograms of S80T20 by thermal treatment time at 140 °C.

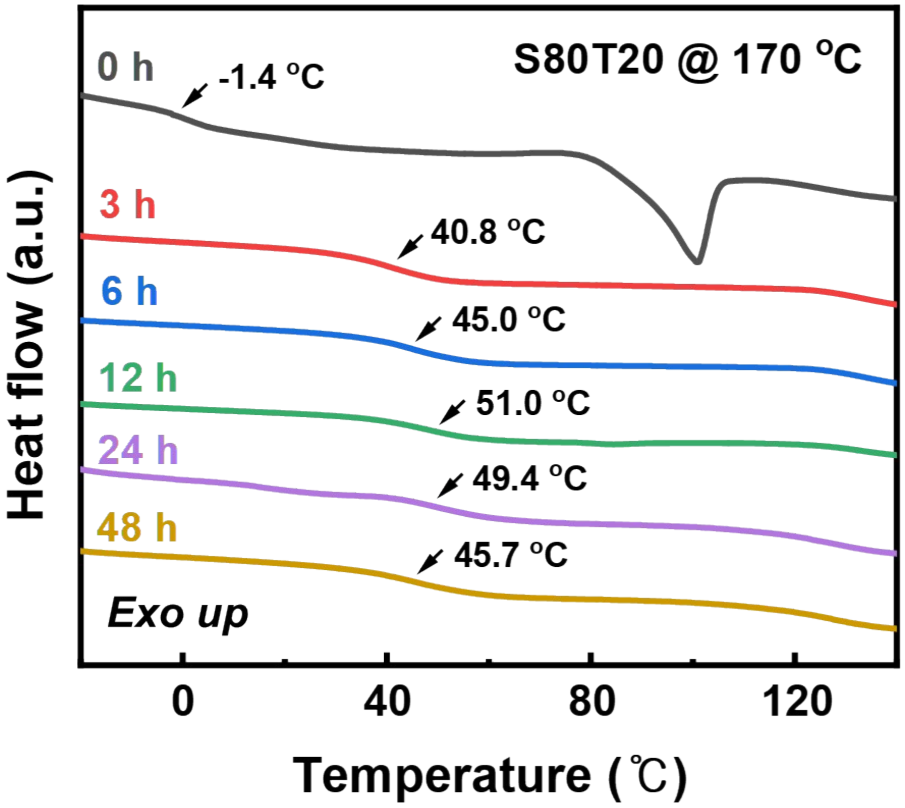

Fig. S7. DSC thermograms of S80T20 by thermal treatment time at 170 °C.

Table S1. Gel fraction values of S80T20 thermally treated at 110, 140, and 170 °C for 3, 6, 12, 24 and 48 h, respectively.

Thermal treatment time (h)	f_g[a]		
	110 ℃	140 ℃	170 ℃
0	0.68	0.68	0.68
3	0.69	0.85	0.91
6	0.79	0.93	0.95
12	0.86	0.99	0.99
24	0.86	0.99	0.99
48	0.89	0.99	0.99

[a]Gel fraction from toluene solvent extraction.

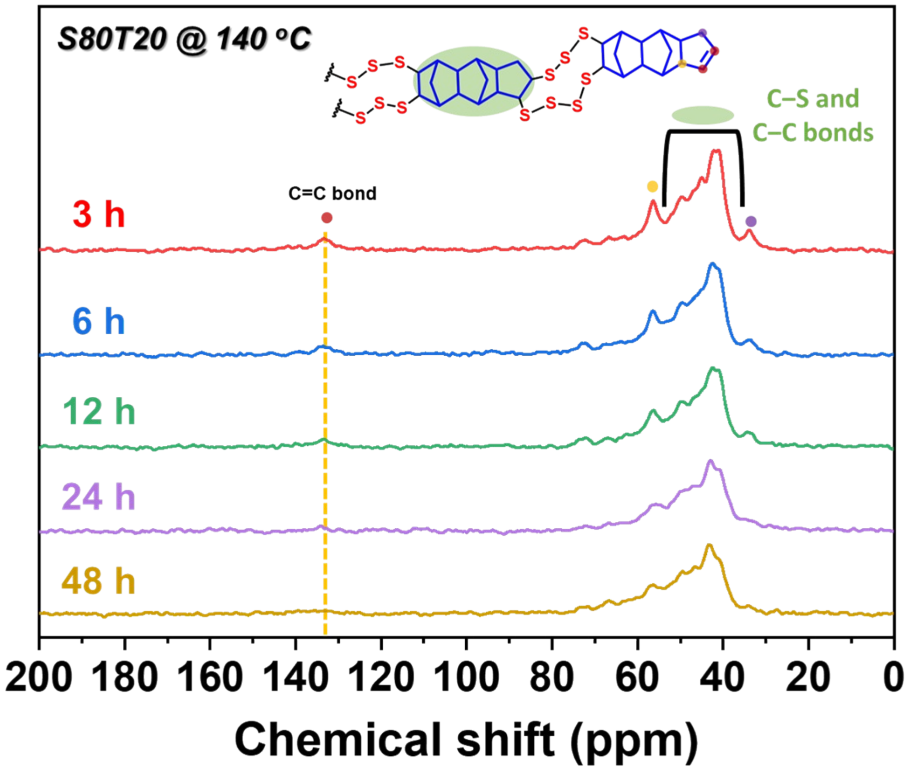

Fig. S8. ^{13}C CP-MAS NMR spectra of S80T20 by different thermal treatment time at 140 °C and expected chemical structure with ^{13}C NMR peak assignments.

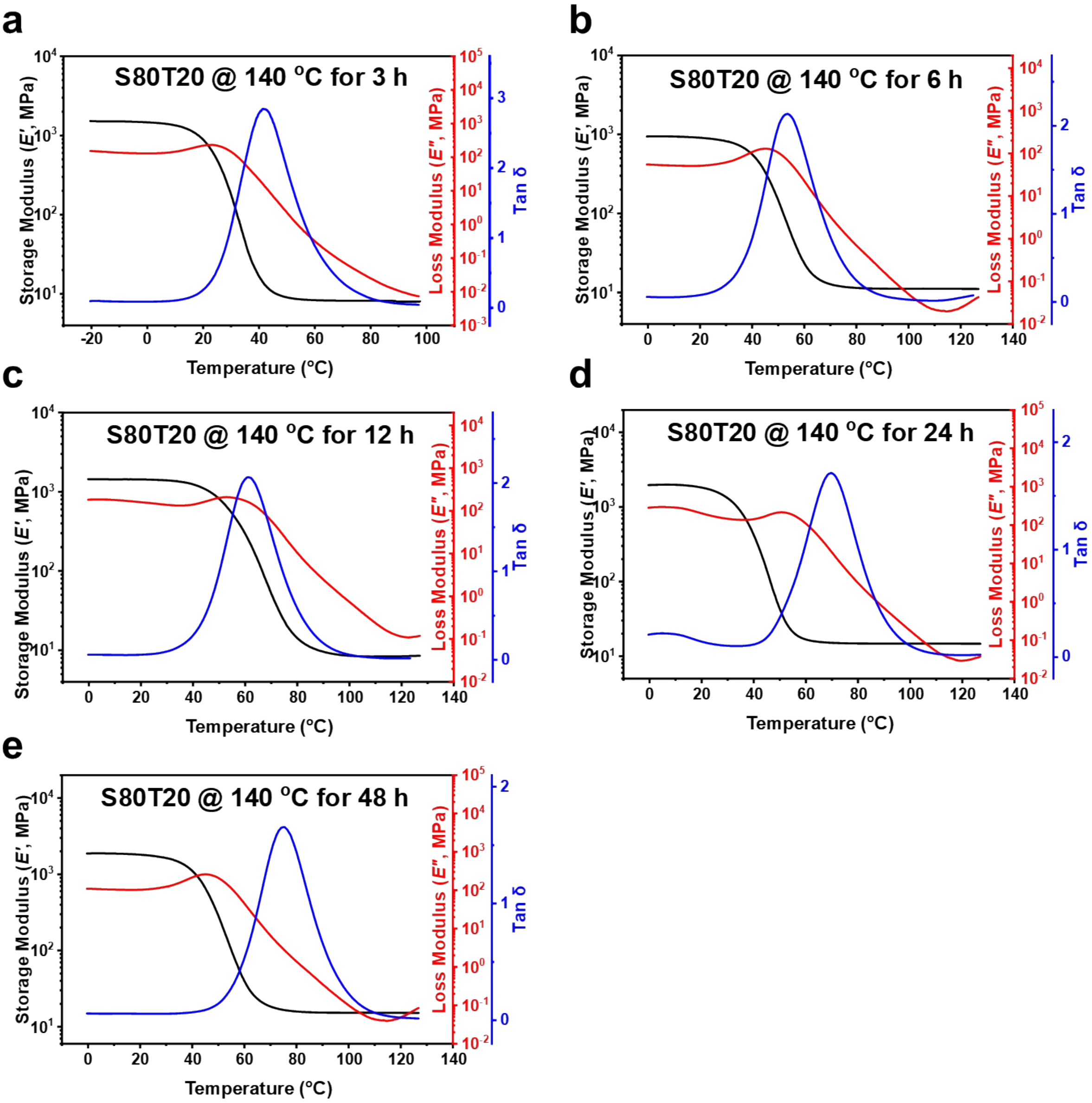

Fig. S9. DMA temperature sweep tests of S80T20 thermally treated at 140 °C for (a) 3 h, (b) 6 h, (c) 12 h, (d) 24 h, (e) 48 h. All tests were conducted under constant frequency of 1 Hz and a heating rate of 3 °C min^{-1}.

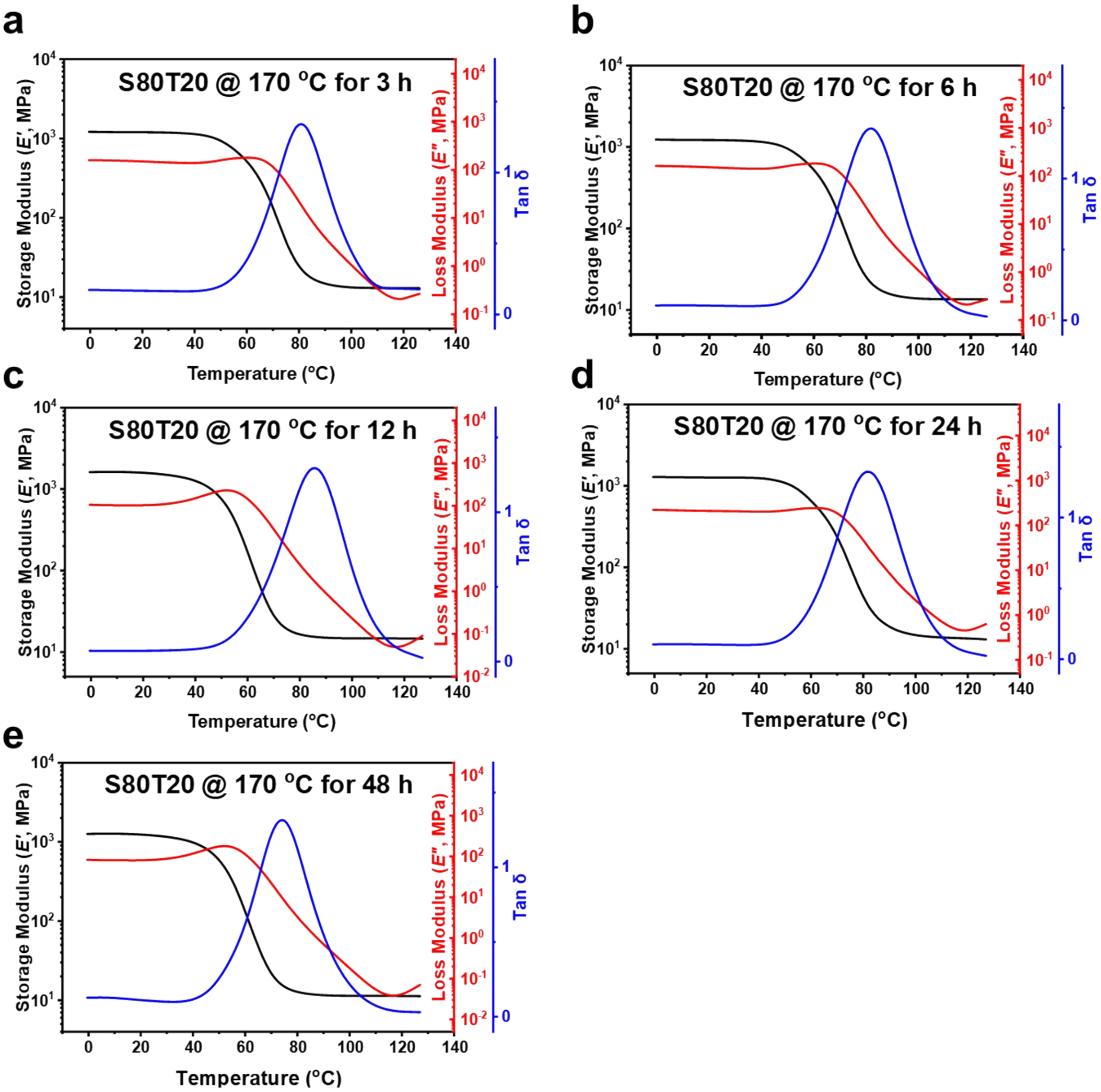

Fig. S10. DMA temperature sweep tests of S80T20 thermally treated at 170 °C for (a) 3 h, (b) 6 h, (c) 12 h, (d) 24 h, (e) 48 h. All tests were conducted under constant frequency of 1 Hz and a heating rate of 3 °C min^{-1}.

Table S2. *E*’ at 25 °C, T_g, Tan δ max, and crosslinking density of S80T20 extracted and calculated from temperature sweep curves of DMA temperature sweep by different thermal treatment conditions.

Thermal treatment time (h)		*E*’ at 25 °C (MPa)	*E*′ high (MPa)	T_g (Tan δ)	v_e (mol/m^{-3})
@ 140 ℃	**3**	490	8.3	41.9	992.1
	6	873	11.9	54.7	1367.7
	12	1,416	13.0	61.4	1466.2
	24	1,646	14.7	69.6	1628.6
	48	1,740	15.3	75.3	1665.9
@ 170 ℃	**3**	1,193	13.2	81.0	1415.0
	6	1,212	13.7	82.2	1463.7
	12	1,542	14.7	85.6	1559.2
	24	1,264	14.4	82.7	1531.6
	48	1,203	11.4	73.9	1249.1

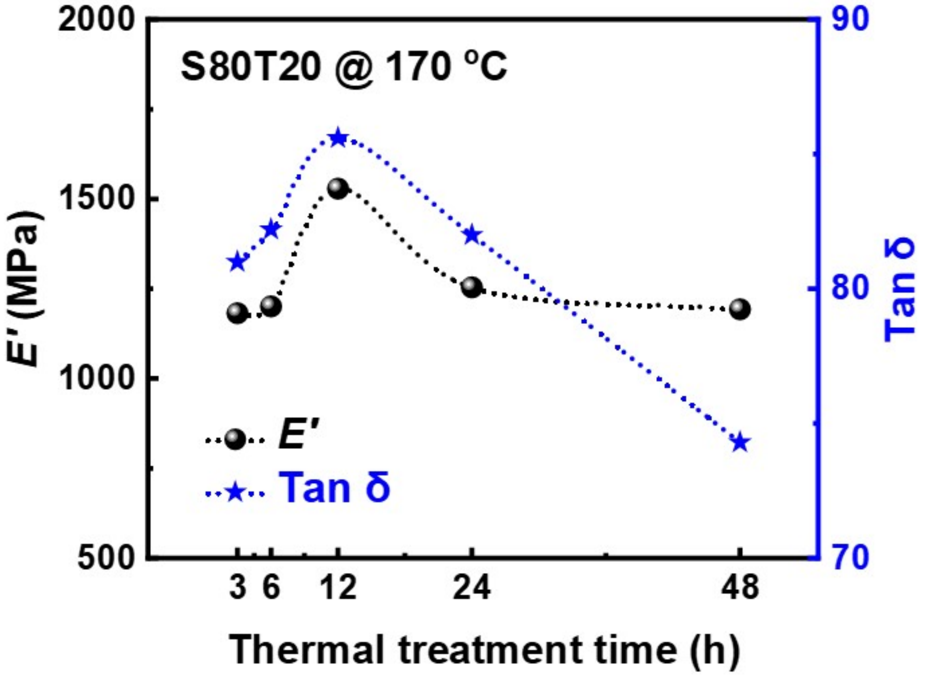

Fig. S11. Rheological properties of S80T20 by thermal treatment time at 170 °C. *E*' values were measured at 25 °C.

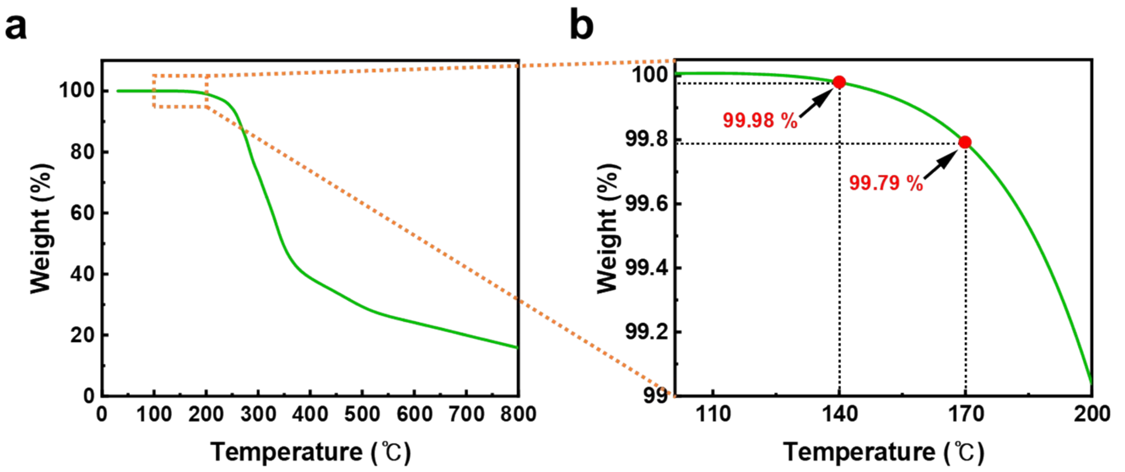

Fig. S12. TGA thermogram of (a) S80T20 and (b) magnified temperature region range from 100 to 200 °C.

Table S3. Elemental analysis of S80T20 by thermal treatment time at 140 °C.

Thermal treatment time (h)	Element (%)			
	Carbon (C)	Hydrogen (H)	Nitrogen (N)	Sulfur (S)
0	15.39	1.28	-	83.32
12	15.65	1.32	-	83.04
24	16.40	1.40	-	82.20
48	16.83	1.44	-	81.73

Table S4. Elemental analysis of S80T20 by thermal treatment time at 170 °C.

Thermal treatment time (h)	Element (%)			
	Carbon (C)	Hydrogen (H)	Nitrogen (N)	Sulfur (S)
0	15.39	1.28	-	83.32
12	15.91	1.42	-	82.67
24	16.66	1.49	-	81.85
48	17.54	1.61	-	79.97

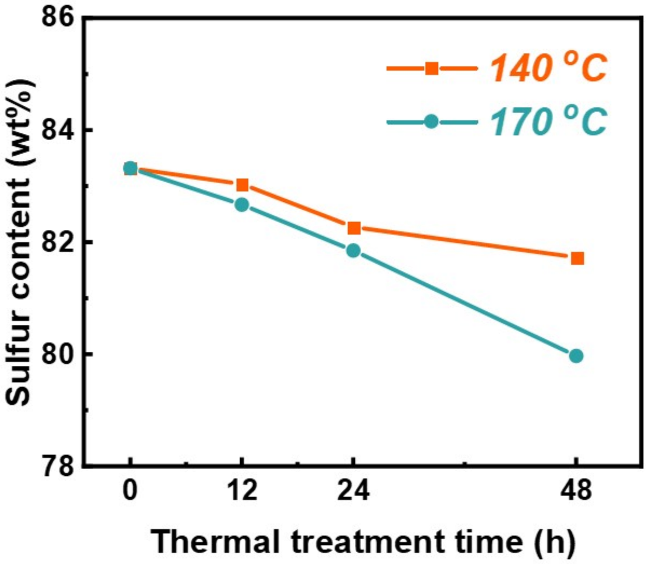

Fig. S13. Sulfur content of S80T20 through the thermal treatment time at 140 and 170 °C.

IR Optical Characterization of thermally treated S80T20

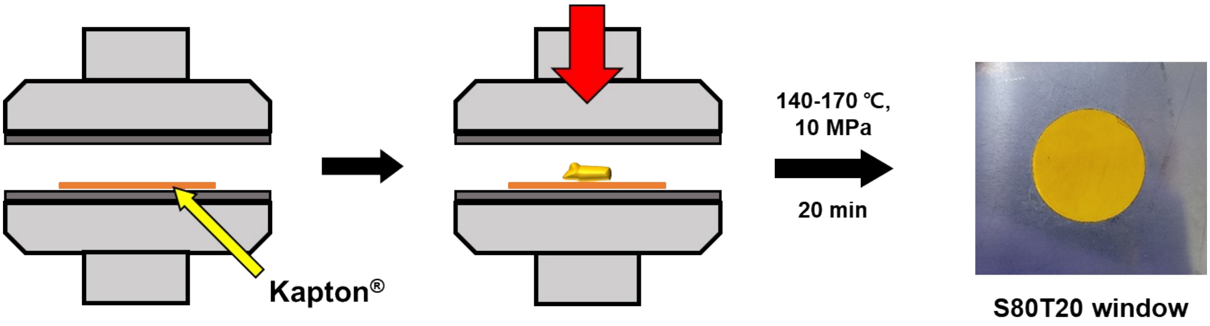

Fig. S14. Schematic illustration for the preparation of S80T20 window *via* hot pressing.

Fig. S15. Digital image of window made from S80T20 thermally treated for 12 h at 140 °C. (Dia. 25 mm × thickness 1 mm). Scale bar for the image is 1 cm.

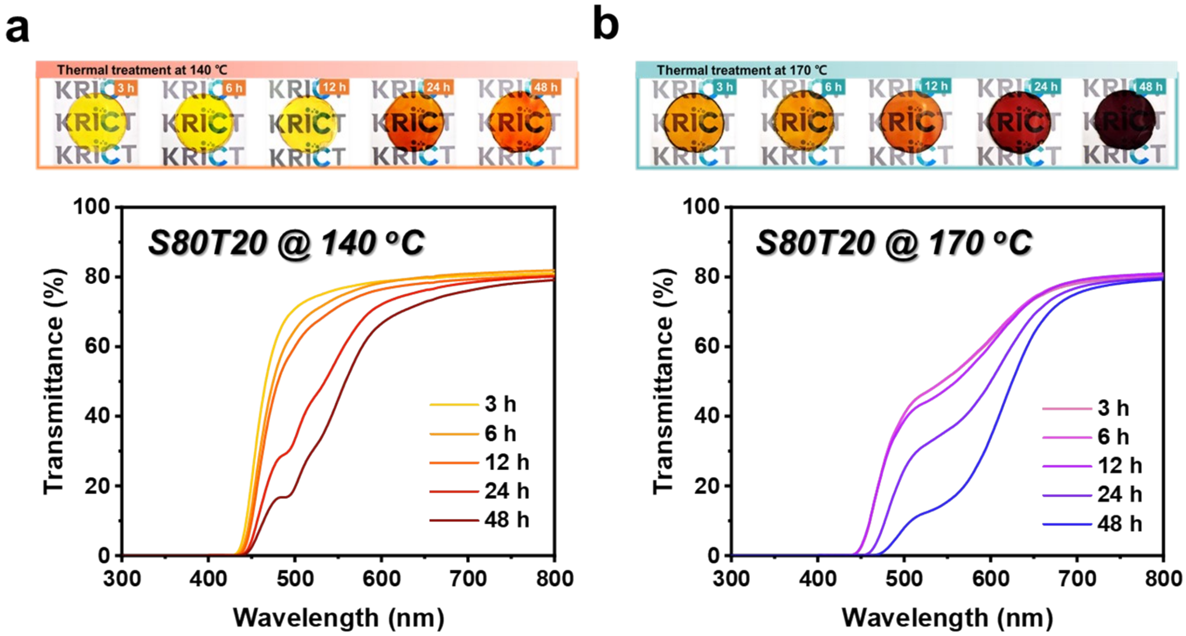

Fig. S16. UV-vis spectra of thermally treated S80T20 at (a) 140 °C and (b) 170 °C.

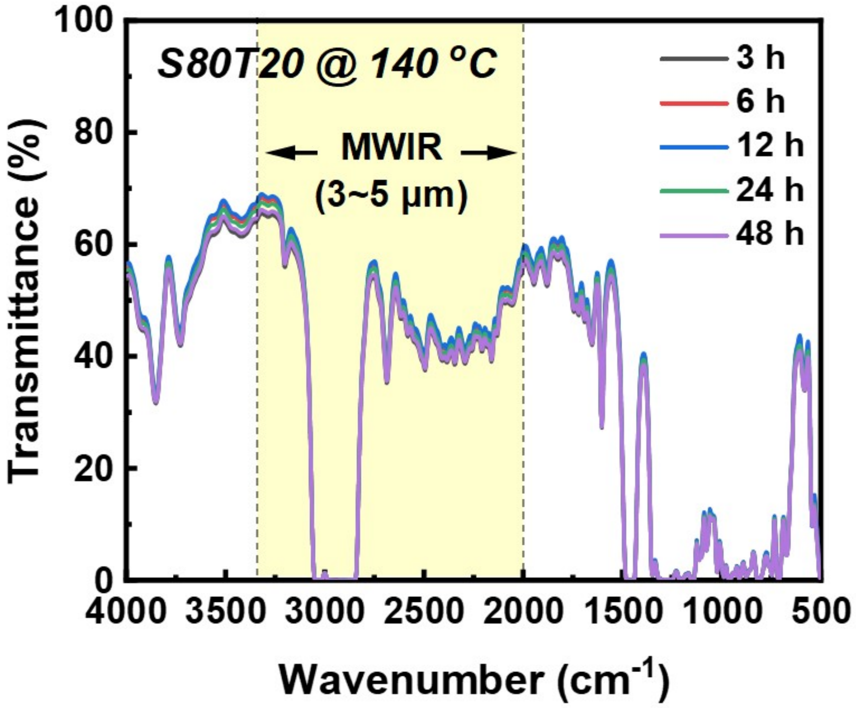

Fig. S17. IR spectra of S80T20 window thermally treated at 140 °C for 3, 6, 12, 24, and 48 h. All transmittance measurements were conducted using 1 mm-thick windows.

Table S5. MWIR transmittance (%T) of S80T20 according to the thermal treatment time at 140 °C. All transmittance measurements were conducted using 1 mm-thick windows.

Thermal treatment time (h)	MWIR Transmittance (%T)
3	38.50
6	40.21
12	41.23
24	39.42
48	38.55

IR transmittance (%) of the mid-wave infrared (MWIR) region (3–5 μm, 3333-2000 cm^{-1}) was calculated from the integration of the transmitted area.

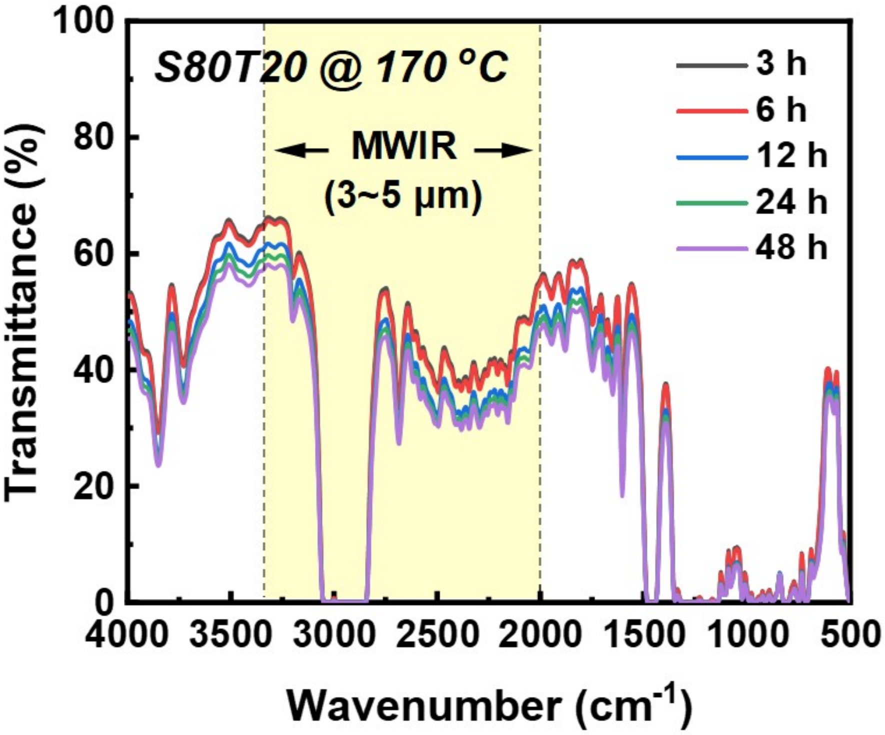

Fig. S18. IR spectra of S80T20 window thermally treated at 170 ˚C for 3, 6, 12, 24, and 48 h. All transmittance measurements were conducted using 1 mm-thick windows.

Table S6. MWIR transmittance (%T) of S80T20 according to the thermal treatment time at

170 °C. All transmittance measurements were conducted using 1 mm-thick windows.

Thermal treatment time (h)	MWIR Transmittance (%T)
3	38.24
6	37.93
12	34.67
24	32.83
48	31.19

IR transmittance (%) of the mid-wave infrared (MWIR) region (3–5 μm, 3333-2000 cm^{-1}) was calculated from the integration of the transmitted area.

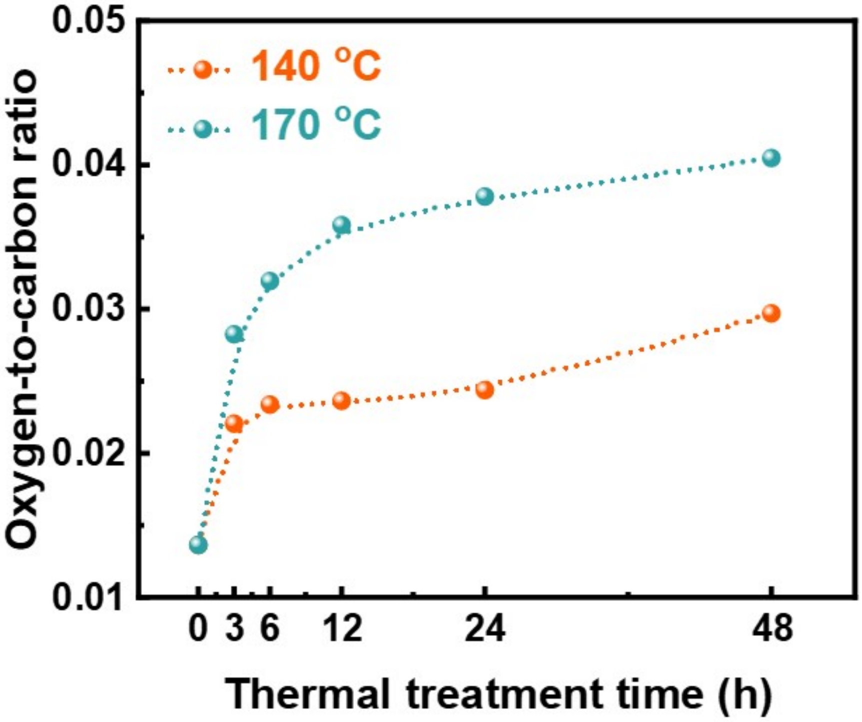

Fig. S19. Oxygen-to-carbon ratio of S80T20 after the thermal treatment under the different conditions, as determined from elemental analysis.

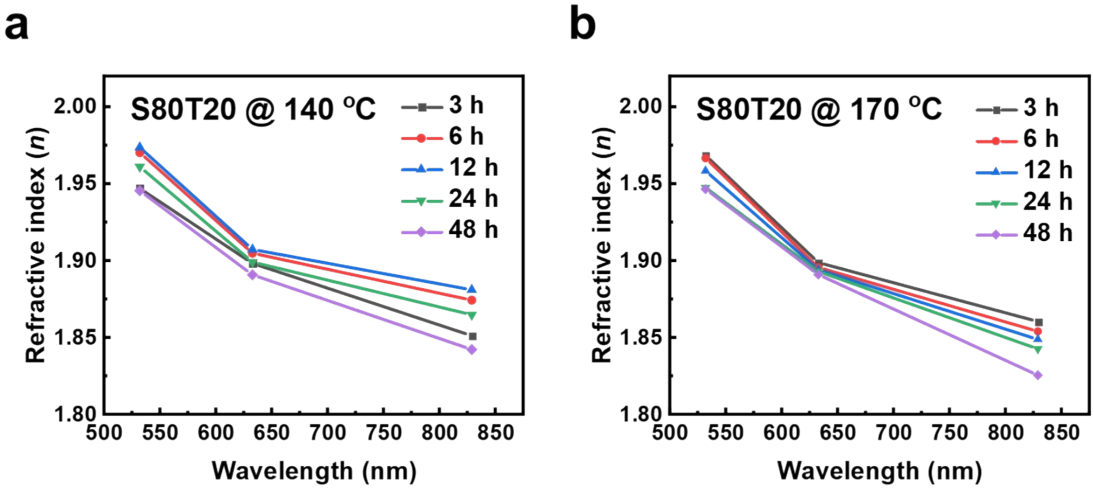

Fig. S20. Refractive indices of S80T20 after thermal treatment at (a) 140 °C and (b) 170 °C, respectively.

Table S7. Refractive indices of S80T20 according to the thermal treatment time at 140 °C.

Thermal treatment time (h)	**Refractive index (*n*)**		
	532 nm	**632.8 nm**	**829 nm**
3	1.947	1.898	1.851
6	1.970	1.905	1.874
12	1.974	1.907	1.881
24	1.961	1.899	1.865
48	1.945	1.891	1.842

Table S8. Refractive indices of S80T20 according to the thermal treatment time at 170 °C.

Thermal treatment time (h)	Refractive index (*n*)		
	532 nm	**632.8 nm**	**829 nm**
3	1.968	1.899	1.860
6	1.967	1.896	1.854
12	1.958	1.894	1.849
24	1.947	1.893	1.843
48	1.946	1.891	1.825

Synthesis and Structural Characterization of S*x*Se*y*T20s

Table S9. Feed ratio of ES, Se, and TCPD for the inverse vulcanization to obtain S72Se8T20, S64Se16T20, and S56Se24T20, respectively.

	Weight (%)				Atom (mol %)			
	S:Se	S	Se	TCPD	S:Se	S	Se	TCPD
S72Se8T20	90:10	72	8	20	95.7 : 4.3	91.74	4.13	4.13
S64Se16T20	80:20	64	16	20	90.8 : 9.2	86.78	8.83	4.39
S56Se24T20	70:30	56	24	20	85.2 : 14.8	81.17	14.13	4.70

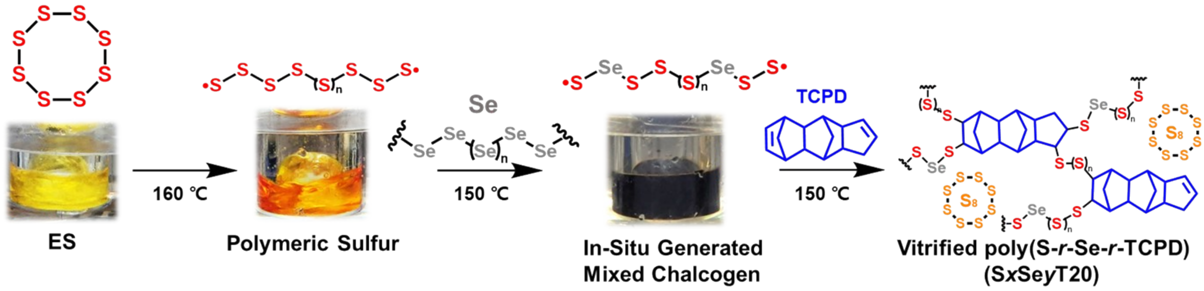

Fig. S21. Synthetic procedures of poly(S_x-*r*-Se_y-*r*-TCPD20)s (S*x*Se*y*T20s).

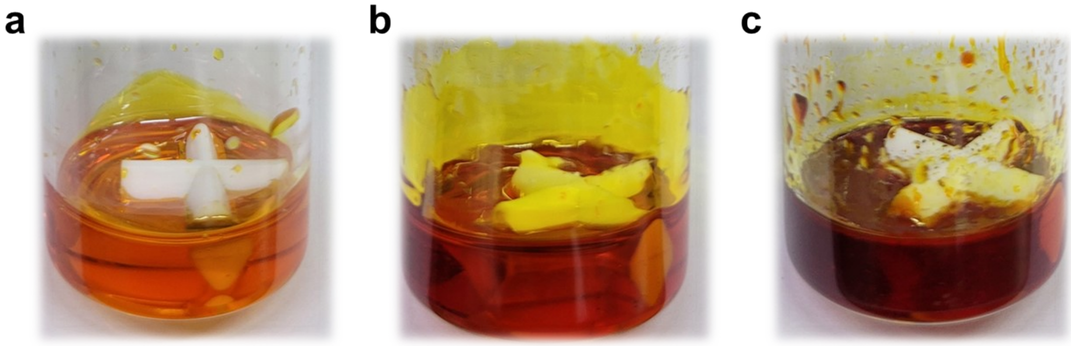

Fig. S22. Digital images of immediately vitrified (a) S72Se8T20, (b) S64Se16T20, and (c) S56Se24T20 immediately after inverse vulcanization.

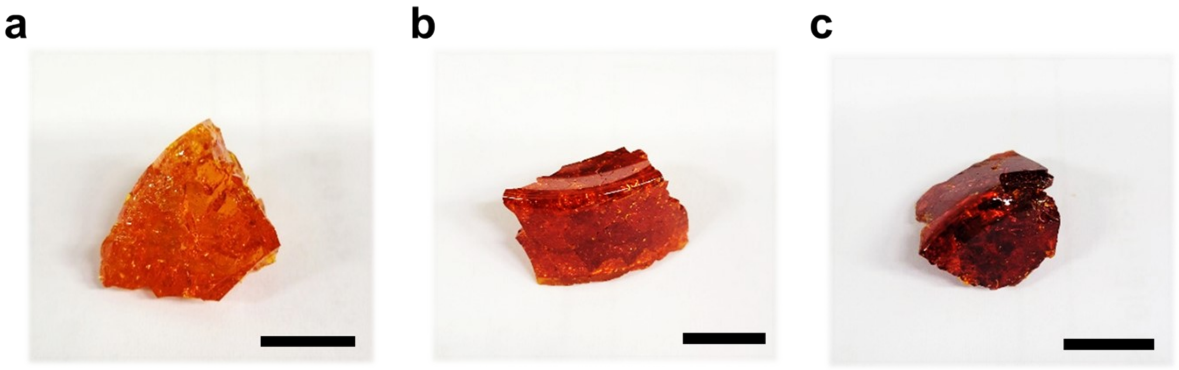

Fig. S23. Digital images of obtained (a) S72Se8T20, (b) S64Se16T20, and (c) S56Se24T20 chunk after quenching in liquid nitrogen. All scale bars for the images are 1 cm.

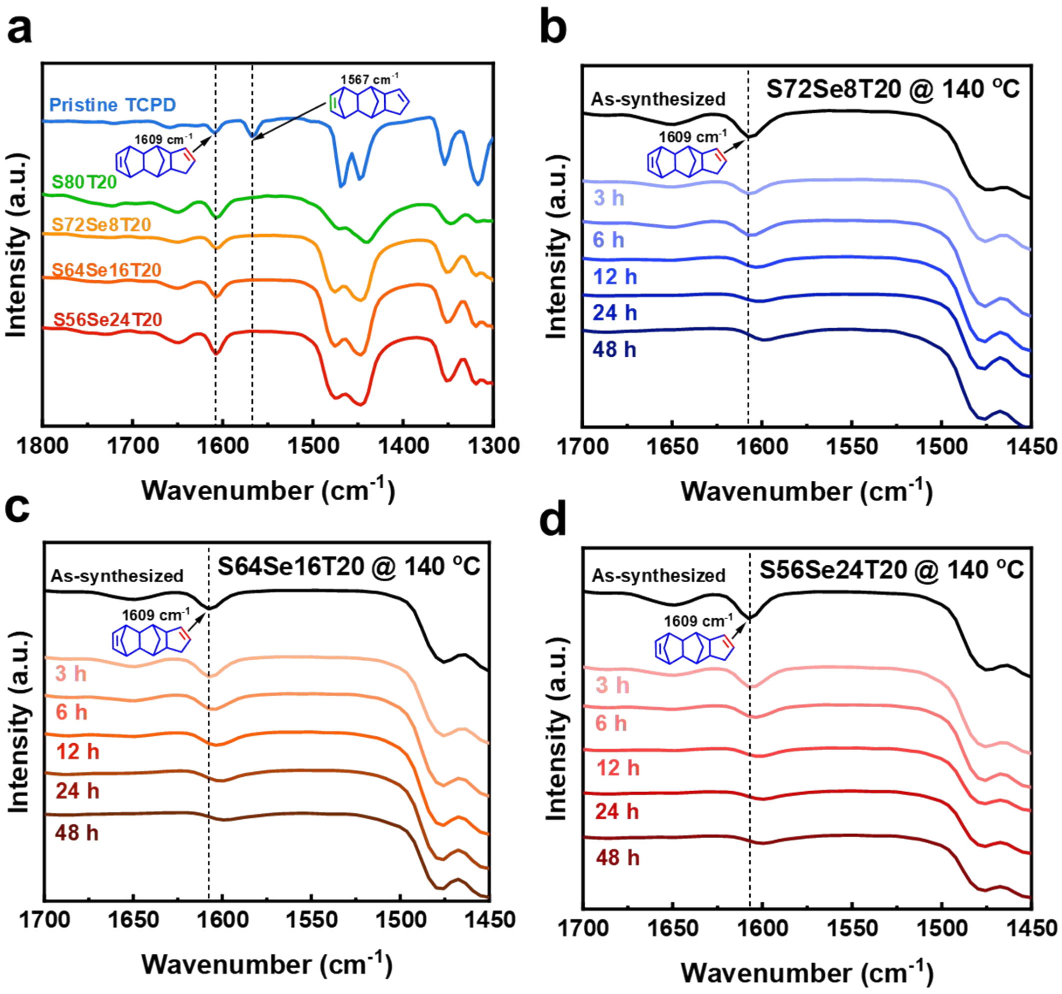

Fig. S24. (a) FT-IR spectra of TCPD and vitrified S80T20, S72Se8T20, S64Se16T20, and S56Se24T20 immediately after inverse vulcanization. FT-IR spectra of (b) S72Se8T20, (c) S64Se16T20, and (d) S56Se24T20 by the thermal treatment time at 140 °C.

Thermomechanical and IR Optical Characterization of thermally treated S*x*Se*y*T20s

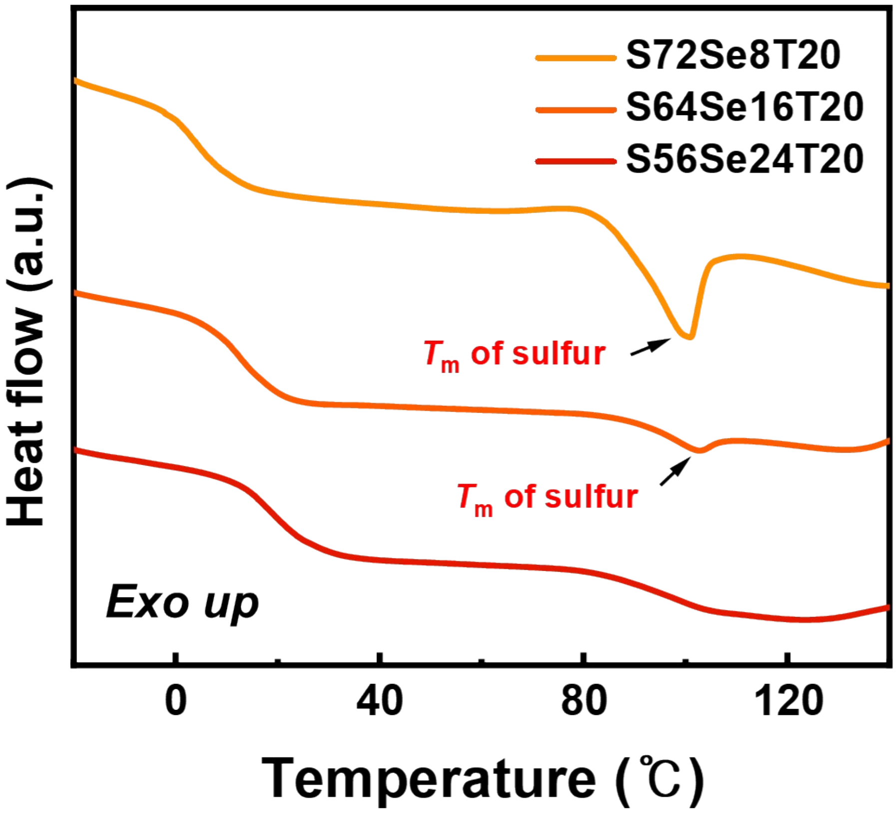

Fig. S25. DSC thermograms of as-synthesized S72Se8T20, S64Se16T20, and S56Se24T20.

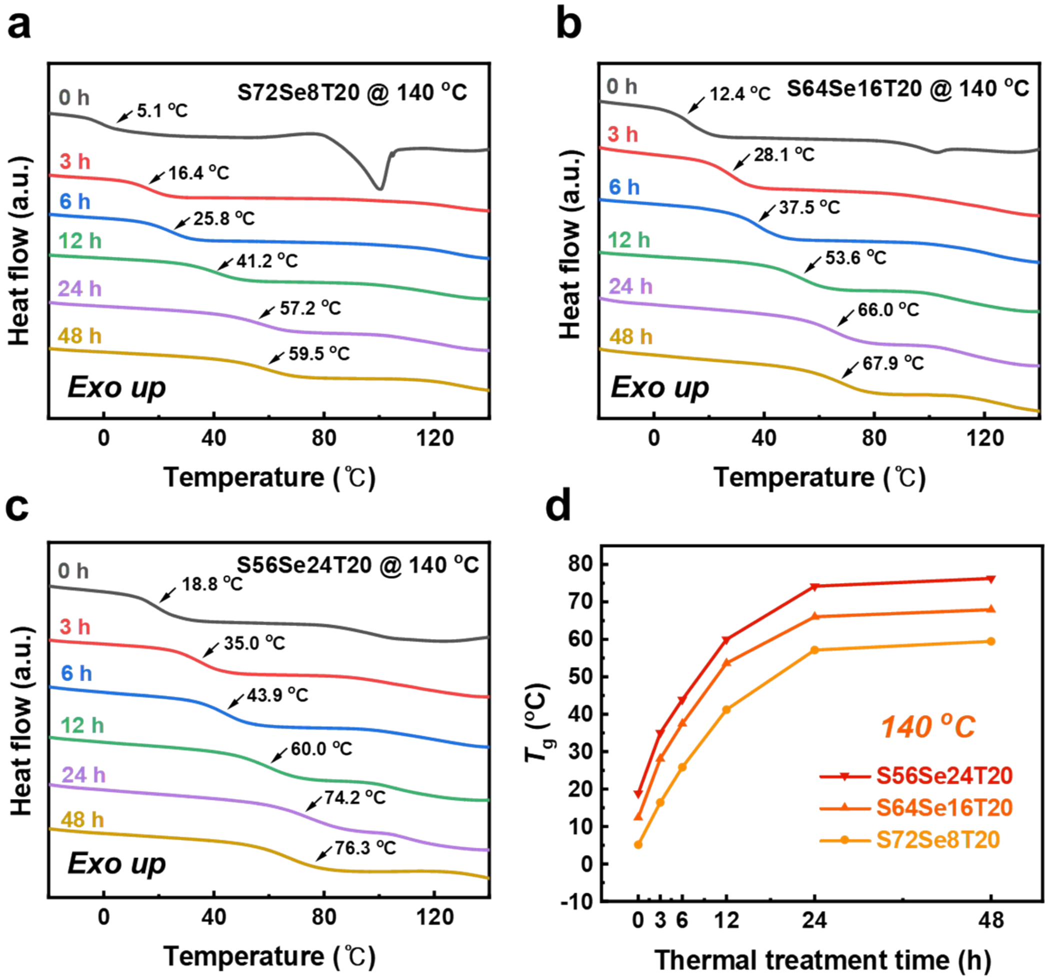

Fig. S26. DSC thermograms of (a) S72Se8T20, (b) S64Se16T20, and (c) S56Se24T20 after the thermal treatment at 140 °C, respectively. (d) T_g trends of S*x*Se*y*T20s according to the thermal treatment at 140 °C.

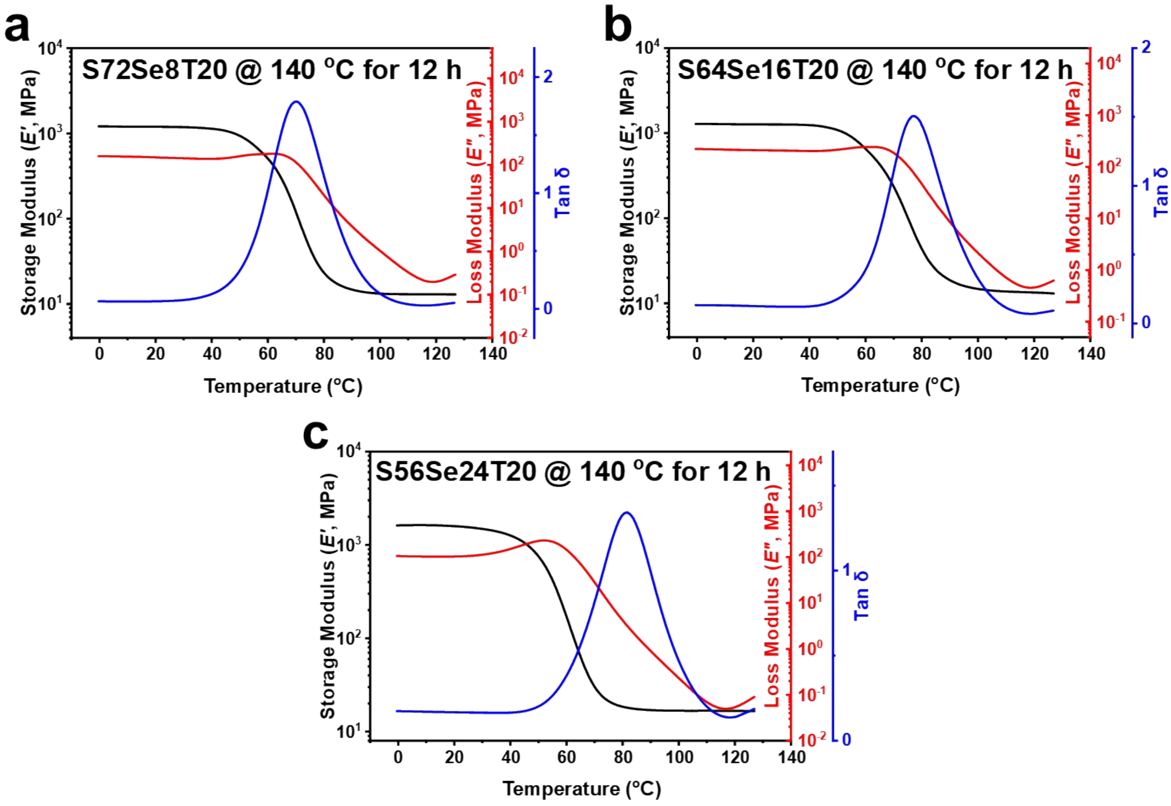

Fig. S27. DMA temperature sweep tests of S*x*Se*y*T20s thermally treated at 140 °C for 12 h. All tests were conducted under constant frequency of 1 Hz and a heating rate of 3 °C min^{-1}.

Table S10. *E*’ at 25 °C, T_g, Tan *δ* max, and crosslinking density of S*x*Se*y*T20s extracted and calculated from temperature sweep curves of DMA temperature sweep by different thermal treatment conditions.

Thermal treatment condition	**Sample**	**E' at 25 °C (MPa)**	**E' high (MPa)**	**T_g (Tan δ)**	**v_e (mol/m^{-3})**
140 ℃, 12 h	S72Se8T20	1193	14.5	70.87	1593.3
	S64Se16T20	1264	15.3	77.24	1659.1
	S56Se24T20	1544	16.7	80.75	1793.8

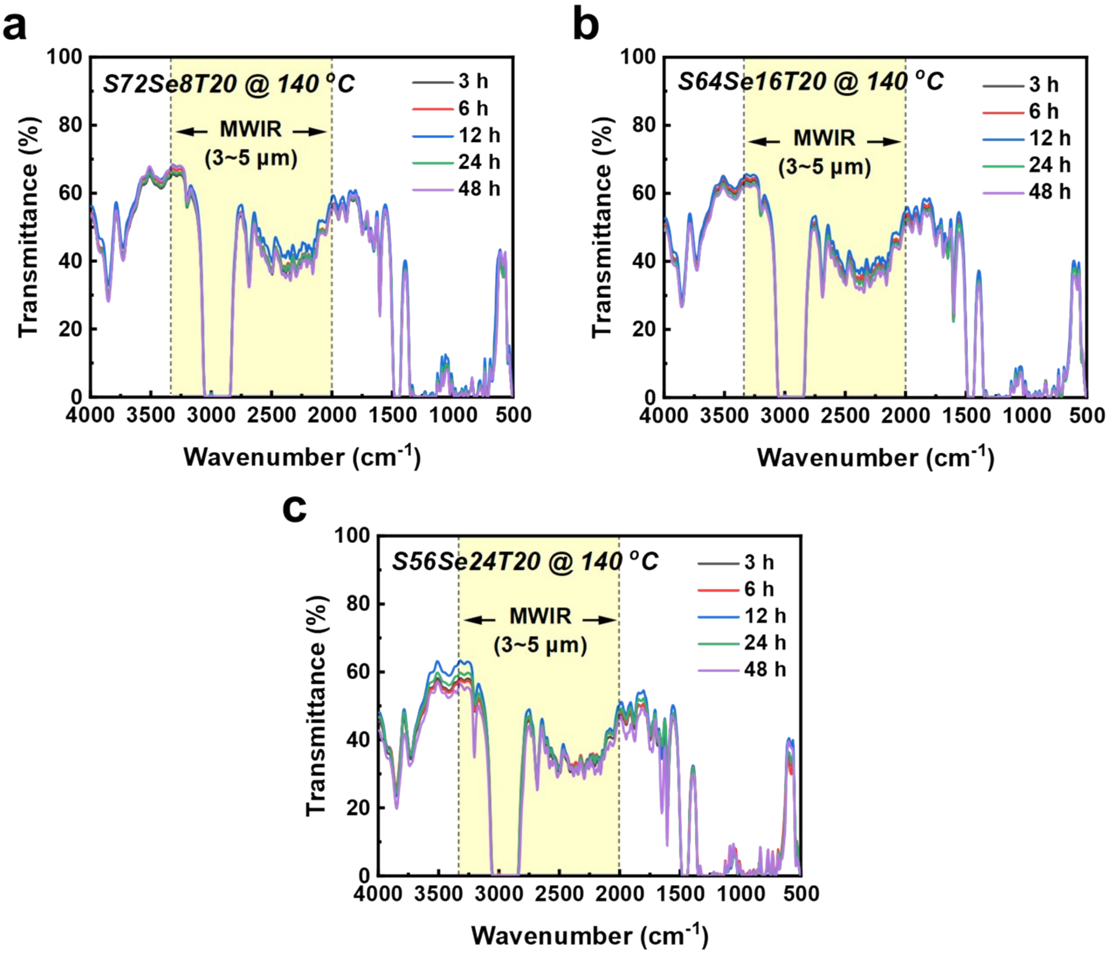

Fig. S28. IR spectra of thermally treated (a) S72Se8T20, (b) S64Se16T20, and (c) S56SeT20 at 140 °C by different treatment time. All transmittance measurements were conducted using 1 mm-thick windows.

Table S11. MWIR transmittance (%T) of S*x*Se*y*T20s thermally treated at 140 ℃ by different treatment time. All transmittance measurements were conducted using 1 mm-thick windows.

	MWIR Transmittance (%T)		
Thermal treatment time (h)	**S72Se8T20**	**S64Se16T20**	**S56Se24T20**
3	37.67	35.95	31.94
6	38.98	37.01	32.58
12	40.67	38.03	33.88
24	38.77	35.09	32.28
48	37.54	34.97	30.63

IR transmittance (%) of the mid-wave infrared (MWIR) region (3–5 μm, 3333-2000 cm^{-1}) was calculated from the integration of the transmitted area.

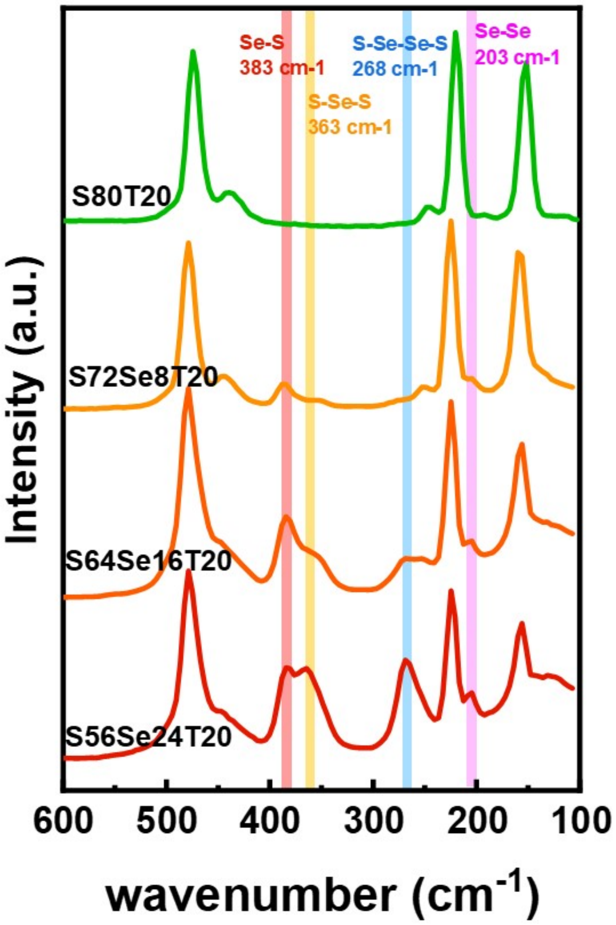

Fig. S29. Raman spectra of S80T20, S72Se8T20, S64Se16T20, and S56Se24T20 after thermal treatment time at 140 ℃ for 12 h.

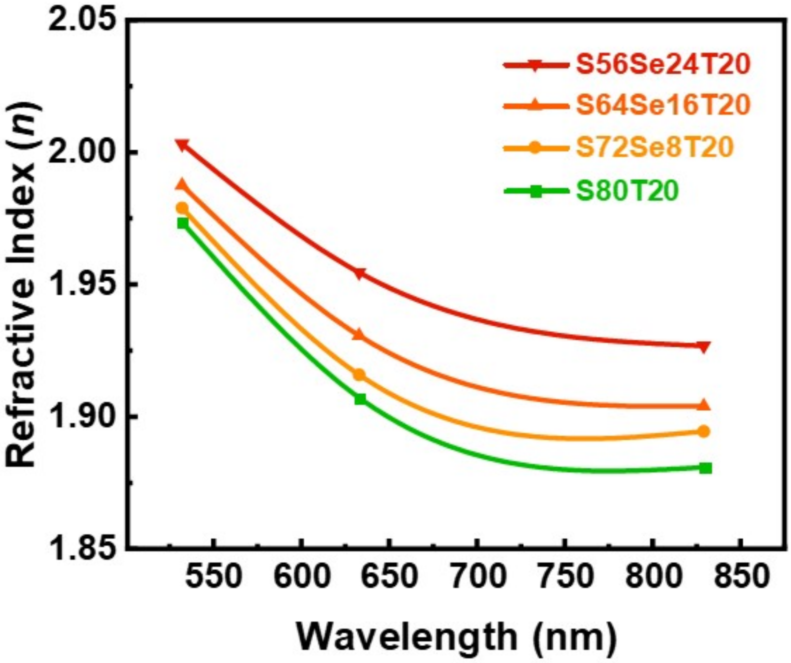

Fig. S30. Refractive index (*n*) of S80T20, S72Se8T20, S64Se16T20, and S56S24T20 after 12 hours of thermal treatment at 140 °C.

Table S12. Refractive index (*n*) measurement of the S80T20, S72Se8T20, S64Se16T20, and S56Se24T20 window after thermal treatment at 140 °C for 12 h.

	Refractive index (*n*)		
	532 nm	**632.8 nm**	**829 nm**
S80T20	1.974	1.907	1.881
S72Se8T20	1.979	1.916	1.895
S64Se16T20	1.988	1.931	1.904
S56Se24T20	2.003	1.955	1.927

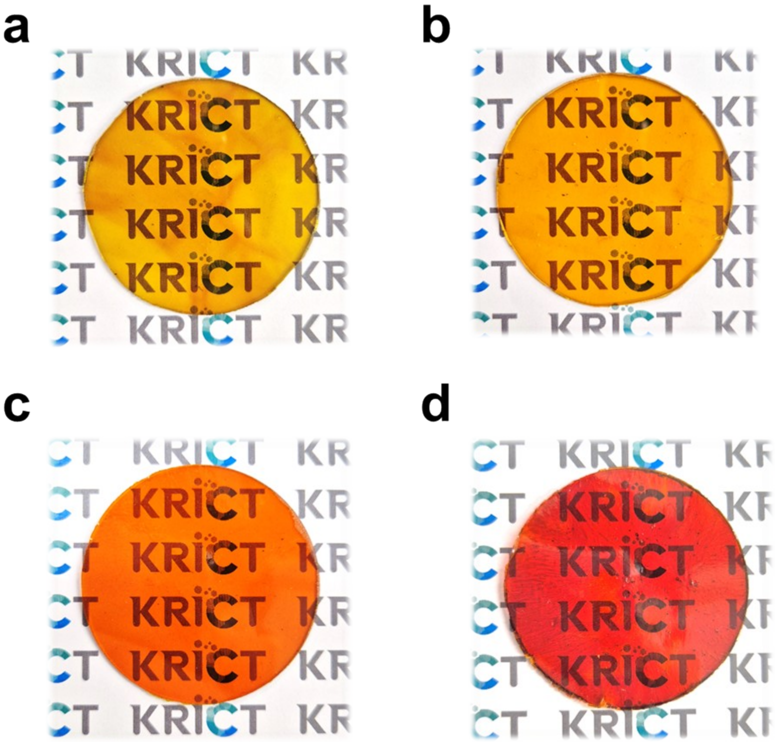

Fig. S31. Digital images of windows (a) S80T20, (b) S72Se8T20 (c) S64Se16T20, and (d) S56Se24T20 windows used for MWIR imaging (diameter 60 mm × thickness ca. 1 mm).

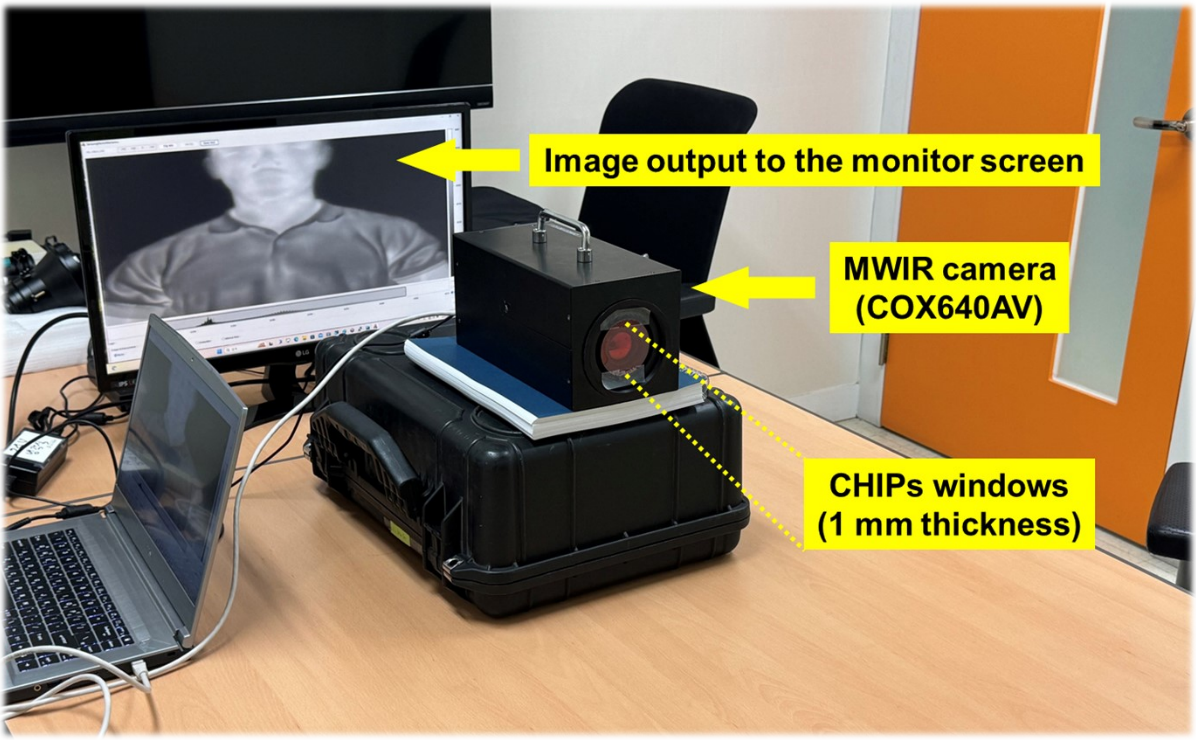

Fig. S32. A photograph of the MWIR thermal imaging setup.

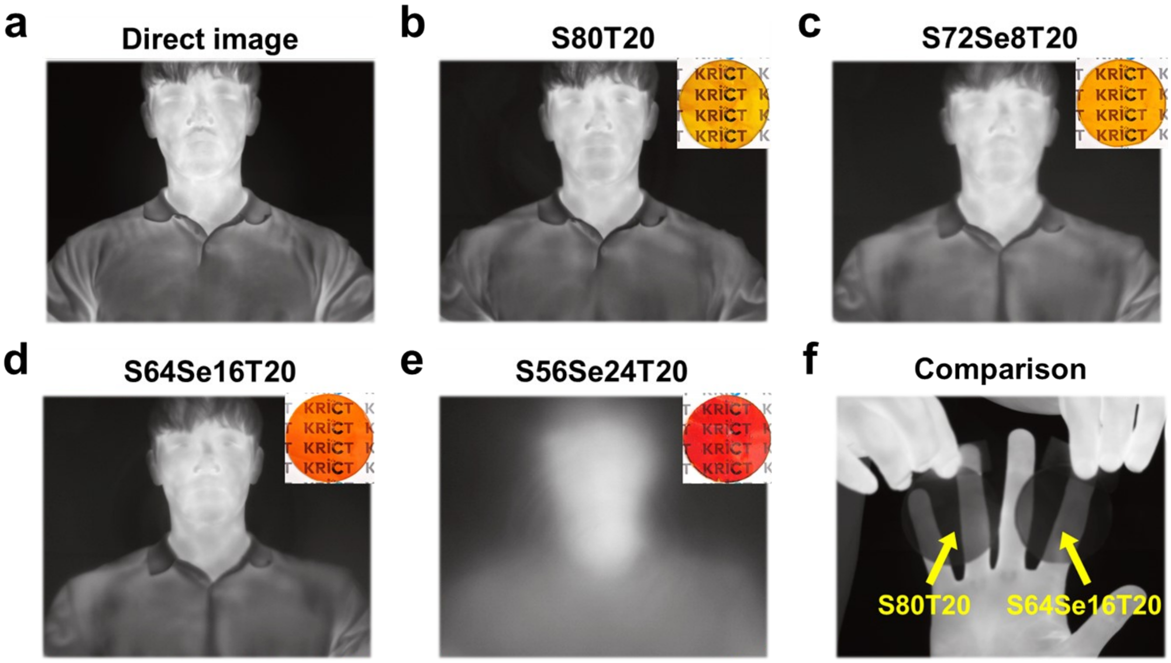

Fig. S33. MWIR thermal images of a male subject were captured (a) without a window sample, through (b) S80T20, (c) S72Se8T20, (d) S64Se16t20, and (e) S56Se24T20 windows. (f) Comparison of the MWIR thermal images of S80T20 and S64Se16T20 windows. The thickness of all windows is 1 mm.

References

1 L. E. Anderson, T. S. Kleine, Y. Zhang, D. D. Phan, S. Namnabat, E. A. LaVilla, K. M. Konopka, L. Ruiz Diaz, M. S. Manchester, J. Schwiegerling, R. S. Glass, M. E. Mackay, K. Char, R. A. Norwood, J. Pyun, Chalcogenide Hybrid Inorganic/Organic Polymers: Ultrahigh Refractive Index Polymers for Infrared Imaging, *ACS Macro Lett.,* 2017, **6**, 500−504.